

# 變化도에 따른 動的問題의 有限要素解析

## The Moving Finite Element Scheme for Time-Dependent Problems with Large Gradients

김 치 경\*    진 치 섭\*\*  
Kim, Chi Kyung    Jin, Chi Sub

---

### 요 약

彈性體에서 波의 흐름, 層流 그리고 亂流에서 剪斷層과 같은 많은 動的 問題들을 有限要素法 또는 差分法으로 解析할 때 自動分割技法이 問題의 解의 正確도를 크게 향상 시켜왔다. 일정한 速度로 움직이는 熱源은 그 熱源의 內部 그리고 周圍에서 높은 變化도를 發生시킨다. 이렇게 變化도가 심한 부분은 有限要素法으로 解析할 때 적절하고 세밀하게 分割된 要素만이 만족스런 解를 얻을 수 있을 것이다. 本研究에서는 空間-時間 領域에서 變化도의 크기에 따라 시간간격이 任意로 조정되는 自動 시간간격 조정법을 發展시켰다.

### Abstract

Moving mesh technique has been used successfully to improve the accuracy of both finite element and finite difference for a variety of time-dependent problems involving wave flows in elastic beams, shear layers in laminar and turbulent flows. A moving heat source will produce steep gradients of the temperature within and near the region of moving source. Therefore, a properly graded finite element mesh is required for a satisfactory resolution of the field. In this study, an adaptive time-step control scheme of the finite element mesh in the space-time domain for these problems is developed.

**Keywords :** moving mesh technique, time-dependent problems, heat source, time-step control scheme, space-time domain

---

\* University of Alabama(Ph.D)  
\*\* 정회원, 부산대학교 토목공학과 교수

· 본 논문에 대한 토의를 1994년 3월 31일까지 학회로 보내 주시면 1994년 6월호에 토의회답을 게재하겠습니다.

## 1. Introduction

Adaptive mesh techniques are currently receiving increased attention in the literature[1, 2,3,4,5,6,7,8]. In the solution of large scale transient problems that involve phase boundaries during nonequilibrium thermal processes or classical boundary layers, it might be hard to accurately capture fine-scale features by way of the structured mesh configurations characteristic of classical finite difference procedures for treating the temporal variations. Regions of rapid change are embedded in regions where the flow variables vary smoothly. However, the inaccurate representation of these subregions in the numerical solutions may deteriorate the overall accuracy obtained. As these subregions which require a finer gridding are usually not known a priori and /or change position, either a fine grid has to be employed over the whole domain, or adaptive refinement techniques are required. Unstructured meshes of finite element methods facilitate adaptive mesh refinement strategies that prove to be essential in the analysis of the problems mentioned above. Ideally, a finite element computer program should generate its own mesh geometry from a minimum number of geometric parameters. The amount of input data required is minimal, and once the relevant coding has been written and tested the possibility of errors is largely eliminated. On the other hand, it may be difficult to devise a suitable algorithm for mesh generation, and few attempts have been made to develop general methods. Particular forms of meshes can, however, be readily generated for simple boundary shapes and can then be modified to suit a wide range of problems. Unstructured meshes are used in the vicinity of large temporal rates of change without

requiring small time steps to be used everywhere.

## 2. Discretization of Time Slab with an Unstructured Mesh

The domain of the time-slab is formulated with the finite element representation by employing the Galerkin approach. Two-dimensional three-node triangular elements in space and time are used to discretize the time slab. In the linear, two-dimensional case, the temperature field  $u^e(x,t)$  in an element is represented by the equation

$$u^e = \alpha_1 + \alpha_2 x + \alpha_3 t \quad (1)$$

Substituting nodal temperatures and coordinates into this equation to solve for the constants  $\alpha_1, \alpha_2, \alpha_3$  and then substituting back into Equation(1) gives the temperature distribution for an element in terms of the shape functions and the nodal values as,

$$u^e(x,t) = \sum_{i=1}^3 N_i(x,t) u_i \quad (2)$$

where,

$$N_i(x,t) = \frac{1}{2A} [a_i + b_i x + c_i t], \quad i=1, 2, 3 \quad (3)$$

and,

$$a_i = x_j t_k - x_k t_j, \quad b_i = t_j - t_k, \quad c_i = x_k - x_j \quad \text{for } j, k=1, 2, 3 \quad (4)$$

with  $x_j, t_j$  the nodal coordinates and  $A$  is the surface area of the element in space time. Using the weighted residual process in which the weighting functions are the shape functions defining the approximations, the

Galerkin method for the heat conduction problem gives

$$\int_{G^e} \left[ \frac{\partial}{\partial x} \left( \kappa \frac{\partial u^e}{\partial x} \right) - \rho c_p \frac{\partial u^e}{\partial t} + f \right] N_i dG^e = 0, \quad i=1, 2, 3 \quad (5)$$

where  $G^e$  is the finite element domain. Evaluating the integrals after inserting the temperature approximation  $u^e = \sum_{i=1}^3 N_i u_i$  results in

$$[g] \{u\} + \{q\} = 0 \quad (6)$$

where

$$[g] = \int_{G^e} \left( \kappa N_{i,x} N_{j,x} + \rho c_p N_i N_{j,t} \right) dG^e - \int_{\Gamma^e} n_x \kappa N_i N_{j,x} d\Gamma^e \quad (7)$$

$$\{q\} = \int_{G^e} f N_i dG^e \quad (8)$$

### 2.1 Calculation of the Temperature Time Rate of Change

To evaluate the time gradients of temperature at each time level, it is necessary to consider the standard procedure of using finite elements in space. The procedure here is a semidiscretization using the Galerkin's residual method. We consider a generic element for the Galerkin formulation. Assuming linear approximation for an element as in Equation(2), we have

$$u^h(x,t) = \sum_{i=1}^2 N_i(x) u_i(t) \quad (9)$$

where  $N_i$  are the usual shape functions defined piecewise, element by elements;  $u_i$  are the time dependent nodal values of  $u(x,t)$ . Now according to Galerkin's method

$$\int_{x_1}^{x_2} \left[ \frac{\partial}{\partial x} \left( \kappa \frac{\partial u^h}{\partial x} \right) - \rho c_p \frac{\partial u^h}{\partial t} + f \right] N_i dx = 0, \quad i=1, 2 \quad (10)$$

Integrating by parts of the first term and substituting of  $u^h = \sum N u$  leads to

$$\begin{aligned} & \kappa \sum_{i=1}^2 \int_{x_1}^{x_2} N_{j,x} N_{i,x} u_i dx + \rho c_p \sum_{i=1}^2 \int_{x_1}^{x_2} N_j N_i u_{i,t} dx \\ & = \int_{x_1}^{x_2} f N_i dx + \kappa u_{,x} N_i \Big|_{x_1}^{x_2}, \quad j=1, 2 \end{aligned} \quad (11)$$

This equation can be written in the simplified form,

$$[k] \{u\} + [c] \{\dot{u}\} = \{q\} \quad (12)$$

where  $[k]$  is known as the conductivity matrix,  $[c]$  is called the capacitance matrix, and  $\{q\}$  is the heat input vector.  $\{\dot{u}\}$  is the vector of time derivatives of the unknown temperature in  $\{u\}$ . Therefore, the gradient of solution can be obtained as

$$\{\dot{u}\} = [c]^{-1} [\{q\} - [k]\{u\}] \quad (13)$$

This expression is used to evaluate the nodal values of the time rates of temperature at the beginning and end of a time-slab that are used in the adaptive mesh generation.

### 3. Mesh Scheme

A mesh moving technique that has been developed is simple and efficient to discretize solutions of the partial differential equation. At each time-step, it uses the node locations and the nodal values of an error indicator, such as the solution gradient to control the motion of the mesh. As time evolves, the mesh can move, change size, or change orientation. At each time-step, new meshes can be

created and old ones vanish. A mesh change is performed at every  $n$  time steps, depending on the solution gradients calculated.

Figure 1. illustrates a mesh scheme for discretizing a time slab when it is anticipated that the locations of maximum (both space and time) gradients lie along a line AB. This would be the case if a wave were travelling in a rod at a constant speed or if an external heat source were moving along the rod with a constant velocity (this will be the test case illustrated later). Along such a principal line the mesh should be characterized by small elements in both space and time dimensions. The elements of the mesh shall be larger the further they are away from this line. It should be noted that once having established this principal line, the domain is divided into two subregions. The principal line is divided by  $n_1^s$  nodes into  $n_1^s - 1$  sides of equal length  $l_0$ . Meshing is performed in the left portion first and then the right portion is done in the same manner. A line parallel to line AB is established at a distance  $l_0$  to the left along the bottom of the time slab. This sliding line is divided by  $n_2^s$  nodes where

$$n_2^s = n_1^s - N \quad (14)$$

with  $N$  equal to a small integer (usually in the range 2 to 4) so that the length of the sides of the elements along this line  $l_1$  are larger than  $l_0$  by a ratio

$$\begin{aligned} d &= l_1 / l_0 \\ &= n_1^s / (n_1^s - N) \end{aligned} \quad (15)$$

This ratio used to expand the layers of elements that are parallel to the line AB. This process continues with each layer being wider

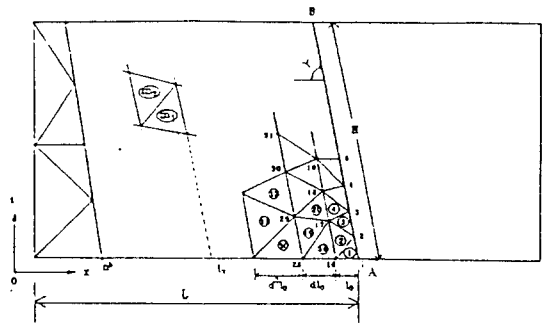


Fig. 1 Meshing Domain

and containing fewer elements than the first layer until the sliding line intersects the left side of the time slab instead of the top. This leaves either a triangular or trapezoidal region that is filled with elements of approximately equal size. This general procedure is repeated in the region to the right of line AB to complete the triangular mesh of elements for the time slab. As the parallel layers approach the ends of the time slab several special cases can be encountered. Special coding has been developed to avoid elements with unfavorable aspect ratios or angles that would cause ill-conditioning in the resulting element matrices.

The accuracy of the solution is significantly affected by the mesh of elements. A good coarse mesh can be produce better numerical results than a finer mesh of ill shaped elements. Two important geometric paramters of a two-dimensional element are the aspect ratio and the largest angle between sides. The aspect ratio is the ratio of the maximum dimension to the minimum dimension of an element. Elements with aspect ratios less than 3 to 1 are known to give good results[8]. If the largest angle between sides to close to  $180^\circ$ , the numerical accuracy deteriorates. Ideally, the interior angles at all vertices in an element will be in the range of  $30^\circ$  to  $120^\circ$ .

### 3.1 Procedure for the Automatic Time Step Control in Space and Time

The mesh in the x-t space will feature general triangular elements and thus the mesh will have non-uniform time steps at each position. The time steps can, in general, will be different for each position along the x-axis. In the case of a moving source(front) in time with a known direction, the grid will be refined locally along the direction of the front to better fit the solution. If there is no information about the direction, maximum gradients of the solution obtained from the each iteration are used to decide the direction. The procedure for the automatic time step control in space and time can be divided into five basic steps.

#### A. Starter time-slab(S.T.S)

Initially, a relatively small time step is used to define a starter time slab in which the elements are just uniform rectangular element in space and time. The results of calculating the solution for this starter time slab are used to set slope of the principal line.

#### B. Locate the point of maximum gradient $u$ on top of S.T.S.

In this step which involves using the results of the first step, the maximum gradients is obtained from the gradient of the solution. Equation(13) is used for the solution gradient calculation.

#### C. Form the first time-slab with an unstructured grid about the front as the principal line.

On the second time-slab with a relatively large time step, we generate a finite element triangulation as described in Section 2. The

small time step is imposed at the position where the steep gradient of the solution exists, and the large time steps are used in those parts where the gradients of the solution is likely to be small so that linear variation will reasonably approximate the time step distribution between the positions. This will allow time steps in regions of large gradient as is normal with only spatial meshes where fine meshes are used in areas of large space gradients.

#### D. Solve for $u$ at $t=\Delta T$ .

The old mesh nodes on the upper boundary corresponding to the previous step must be used as mesh nodes for the lower boundary of the new time-slab domain. As an initial solution for the linear iterations on each time slab we have used the same initial solution for the first time slab with the Dirichlet boundary condition given by the solution on the previous time slab superposed on upper boundary. Therefore, these discrete solutions on the upper boundary will be interpolated linearly and will be used as Dirichlet boundary conditions for next time step.

#### E. Locate the point of maximum gradient $u$ which gives a new slope to the front.

The point of the maximum gradient is selected at the upper boundary. It gives a new direction to the front. Generally this direction is not identical with that of previous direction of the front.

### 3.2 Demonstration of Adaptive Mesh Generation

To illustrate the ability of the mesh to adapt to a moving front, consider the case when the heat source moves with a velocity as specified

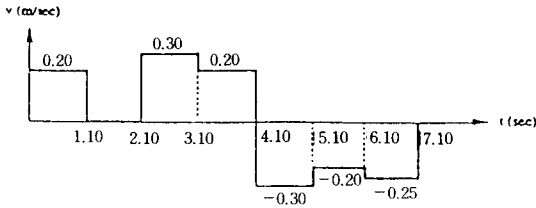


Fig. 2 Velocity history of moving source

in Fig. 2.

This problem shows the mesh refinement technique in the case where the refinement differs from one time-slab to the next. Fig. 3 shows the mesh that was generated for seven time-slab of  $\Delta t=1.0$  second. The moving source is captured inside the fine mesh of elements which are generated along the front. The total number of grid points required (corresponding to time from  $t=0.1$  to  $t=7.1$ ) for this computation would be 4105 which is about 25% of the number of nodes if a uniform refinement would be used and all elements were small enough to adequately model the large spatial and temporal gradients along the front. These results show the adaptive mesh generators capability to produce a efficient mesh for moving front boundary value problems.

#### 4. Problem of a Moving Source

We shall consider the non-stationary temperature field produced in a finite bar whose material is steel. The lateral surface of the bar will be thermally insulated. There is a heat source in a zone of length  $\Delta L$  of the bar which generates heat at a rate given by  $f_0$ . This heated zone starts from the right end of the bar and begins to move toward the left at a constant axial velocity  $v$  along the bar. Before studying the numerical results obtained using

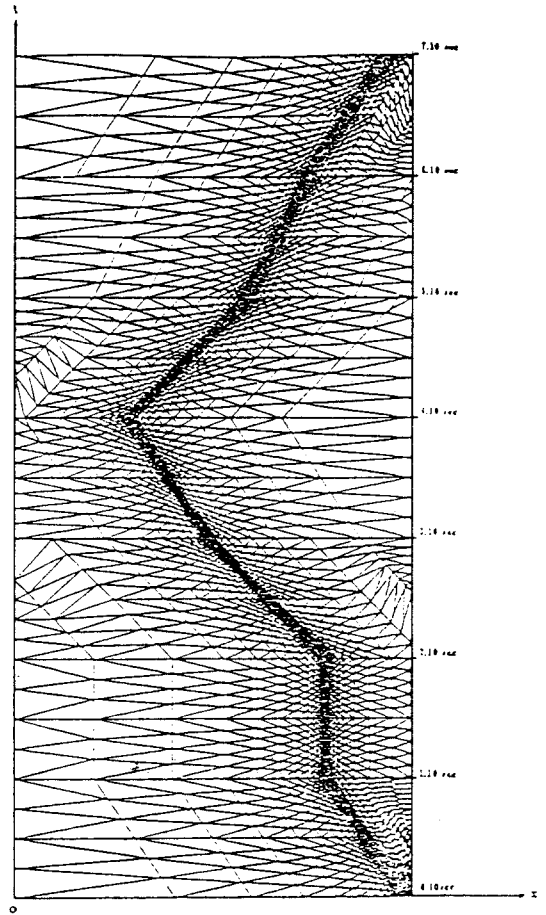


Fig. 3 Finite element mesh of overall time-slab : 4105 nodes, 7732 elements

the space-time finite element formulations, it is instructive to look at the governing equation of the heat conduction problem when the heat source is moving. The problem is characterized by

$$\rho c_p \frac{\partial u}{\partial t} - \kappa \frac{\partial^2 u}{\partial x^2} = f(x, t) \quad (16)$$

The initial and boundary conditions are given by, respectively,

$$\begin{aligned}
 u(x,0) &= u_0 \\
 -\kappa \frac{\partial u}{\partial x}(0,t) &= q_b \\
 -\kappa \frac{\partial u}{\partial x}(L,t) &= h_0(U - u_x)
 \end{aligned}
 \tag{17}$$

The moving heat source is illustrated in Fig. 4. Using unit Heaviside's function  $\eta(x)$ , we can express the heat source as

$$f(x,t) = f_0 [\eta(x - L + vt) - \eta(x - L + vt + \Delta L)]
 \tag{18}$$

where  $f_0$  is a strength of source and

$$\eta(x) = \begin{cases} 1 & \text{for } x > 0 \\ 0 & \text{for } x < 0 \end{cases}$$

Then

$$f(x,t) = \begin{cases} 0 & \text{for } x < L - vt ; \\ f_0 & \text{for } L - vt < x < L - vt + \Delta L ; \\ 1 & \text{for } L - vt + \Delta L < x ; \end{cases}
 \tag{19}$$

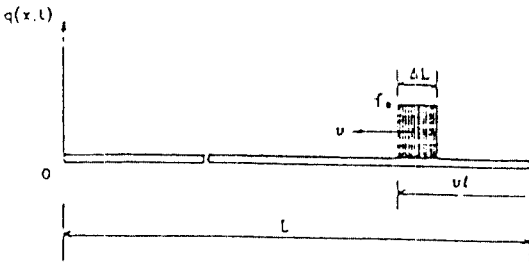


Fig. 4 Rectangular-shaped heat source of width  $\Delta L$  moving at a constant velocity  $v$

This is a linear problem for which there exists an analytical solution in series form. The series solution for temperature  $u(x,t)$  has been derived in the appendix. The following gives the dimensions and material properties used to obtain both the series and Galerkin time-discontinuous numerical results presented later.

- \* Initial condition :  $u(x,t=0) = 50^\circ\text{C}$
- \* Bulk fluid temperature :  $u = 50^\circ\text{C}$
- \* Density :  $\rho = 7875 \text{ kg/m}^3$
- \* Conductivity :  $k = 144.5 \text{ cal/m} \cdot \text{sec}^\circ\text{C}$
- \* Time step of time slabs :  $\Delta t = 1.0 \text{ sec}$
- \* Length of source :  $\Delta L = 0.02 \text{ m}$
- \* Velocity of source :  $v = 0.2 \text{ m/sec}$
- \* Heat flux :  $q = 0 \text{ cal/sec} \cdot \text{m}^2$
- \* Heat coefficient :  $h = 14500 \text{ cal/m}^2 \cdot \text{sec}^\circ\text{C}$

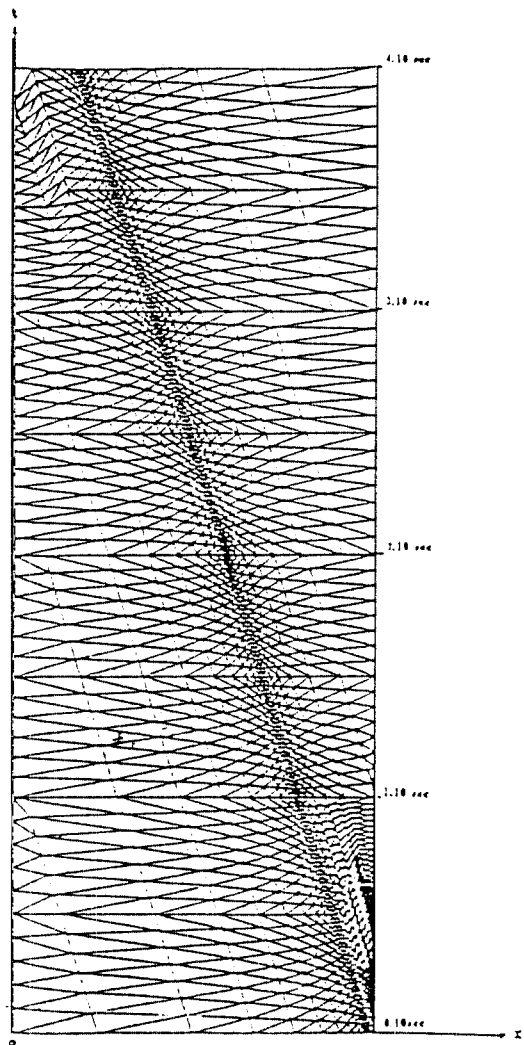


Fig. 5 Space-time finite element mesh

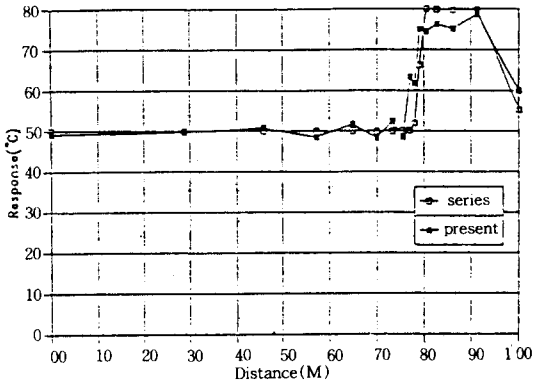


Fig. 6 Comparison of temperature distribution at  $t=1.10$  sec

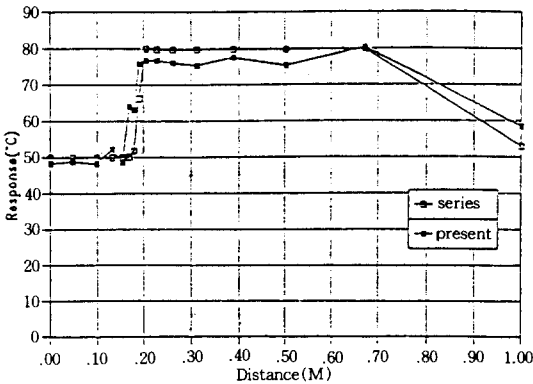


Fig. 7 Comparison of temperature distribution at  $t=4.10$  sec

- \* Specific heat :  $c_p=103$  cal /kg °C
- \* Source intensity :  $f=2.4 \times 10^8$  cal /  $m^3 \cdot$  sec
- \* Length of bar :  $L=1.0$  m
- \* Space step for first step :  $\Delta x=0.01$  m
- \* Time step for S.T.S :  $\Delta t=0.1$  /sec

## 5. Discussion and Conclusion

The solution of this problem is carried out with a starter time slab with  $\Delta t=0.1$  second and then four time slabs  $\Delta t=1.0$  second. The space-time finite element mesh for the four large time slabs is shown in Fig. 5. The

time-discontinuous Galerkin finite element produce temperature distribution at the end of each time slab. These results are plotted in Fig. 6 and 7 respectively. Also shown in these figures are temperature distributions calculated from the series solution.

The numerical results from the time-discontinuous Galerkin finite element method generally agree with the series solution as shown Fig. 6 and 7. At the top of a time slab there are 16 nodes. This indicates the level of spatial discretization. In comparison, the series solution required 200 terms to produce these results. Thus the level of discretization in the finite element method is significantly less. Because of this the sharp rise of temperature in the finite element results induces a fairly high level of oscillation (about 7%). This oscillation is also evidenced in the oscillation in the region to the left of the front (forerunners) and behind the front (tails). Both forerunners and tails tend to oscillate hard when a low level of discretization is used. If series solution had included 15~20 terms then significant oscillation, forerunners, and tails would have been present in the series solution. These results suggest that even finer elements are needed to smooth out the oscillation of the finite element solution. Indeed, if more element were used the finite element results would improve. The point of these numerical results is to establish that the developed adaptive mesh generation technique will efficiently treat moving front problems that occur in many engineering situations.

Numerical results have shown that the adaptive gridding scheme is effective in localizing oscillations due to the sharp gradients or discontinuities in the solution. In this method, we utilize the efficiency of finite elements by choosing a finite element mesh in



the space-time domain where the finite element mesh has been adjusted to steep gradients of the solution both with respect to the space and the time variables. In this way we solved all the difficulties with the classical approach. The gridding is employed in conjunction with a triangular finite element discretization in two dimensions. The grid is adapted at every  $n$  time step, depending on the gradient computed. The guidelines for grid optimization suggested here appear in a form that is attractive for computations and can lead to good improvements in the quality of the finite element solution with relatively small effort. Numerical examples taken from practical moving source problems indicate that with the present approach saving factors in the both CPU and storage requirements of more than an order of magnitude as compared to uniform refinement are attainable, without deteriorating the accuracy of the solution. The space-time finite element method shows considerable potential as an approach to solve the problems. As a example of application of this problem for the concrete, the front of phase change can be considered as a good moving heat source when the concrete is curing. When the concrete is drying in common temperature, the hydraulic heat occuring due to the change of condition from liquid to solid is moving as time ellapse.

#### References

1. Adjerid, S. and Flaherty, J.E., "A moving fi-

- nite element method with error estimation and refinement for one-dimensional time dependent partial differential equations", *SIAM Journal on Numerical Analysis*, 23, 778-796 (1986).
2. Arney, D.C. and Flaherty, J.E., "A two-dimensional mesh moving technique for time-dependent partial differential equations", *Journal of Computational Physics*, 67, 124-144 (1980).
3. Devloo, P., Oden, J.T. and Strouboulis, T., "Implementation of an adaptive refinement technique for the SUPG algorithm", *Computer Methods in Applied Mechanics and Engineering*, 61, 339-358 (1987).
4. Eriksson, K., Johnson, C., "Error estimates and automatic time step control for nonlinear parabolic problems I", *SIAM Journal on Numerical Analysis*, 24, 12-23 (1987).
5. Gelinias, R.J., Doss, S.K. and Miller, K., "The moving finite element method : Application to general partial differential equations with multiple large gradients", *Journal of Computational Physics*, 40, 202-249 (1981).
6. Harten, A. and Hyman, J.M., "Self-adjusting grid methods for one-dimensional hyperbolic conservation laws", *Journal of Computational Physics*, 50, 235-269 (1983).
7. Miller, K., "Moving finite elements II", *SIAM Journal on Numerical Analysis*, 18, 1033-1057 (1981).
8. Oliveira, E.R., "Optimization of finite element solutions", *Proc. 3rd. Conf. Matrix Methods in Structural Mechanics*, Wright-Patterson Air Force Base, OH, 1971.

(접수일자 : 1993. 5. 21)